Mon. Not. R. Astron. Soc. **332,** 705–713 (2002)

The intermediate-age open cluster NGC 2158★

Giovanni Carraro,[1]† Léo Girardi[1,2]† and Paola Marigo[1]†
[1]*Dipartimento di Astronomia, Università di Padova, Vicolo dell'Osservatorio 2, I-35122 Padova, Italy*
[2]*Osservatorio Astronomico di Trieste, Via G.B. Tiepolo 11, I-34131 Trieste, Italy*

Accepted 2002 January 14. Received 2001 November 14; in original form 2001 October 16

ABSTRACT

We report on *UBVRI* CCD photometry of two overlapping fields in the region of the intermediate-age open cluster NGC 2158 down to $V = 21$. By analysing colour–colour (CC) and colour–magnitude diagrams (CMDs) we infer a reddening $E(B-V) = 0.55 \pm 0.10$, a distance of 3600 ± 400 pc, and an age of about 2 Gyr. Synthetic CMDs constructed with these parameters (but fixing $E(B-V) = 0.60$ and [Fe/H] $= -0.60$), and including binaries, field contamination and photometric errors, yield a good description of the observed CMD. The elongated shape of the clump of red giants in the CMD is interpreted as resulting from a differential reddening of about $\Delta E(B-V) = 0.06$ across the cluster, in the direction perpendicular to the Galactic plane. NGC 2158 turns out to be an intermediate-age open cluster with an anomalously low metal content. The combination of these parameters, together with the analysis of the cluster orbit, suggests that the cluster belongs to the old thin disc population.

Key words: Hertzsprung–Russell (HR) diagram – open clusters and associations: general – open clusters and associations: individual: NGC 2158.

1 INTRODUCTION

NGC 2158 (OCL 468, Lund 206, Melotte 40) is a rich northern open cluster of intermediate age, located low in the Galactic plane toward the anticentre direction ($\alpha = 06^{\rm h}07^{\rm m}.5$, $\delta = +24°06'$, $\ell = 186°.64$, $b = +1°.80$, J2000), close to M35. It is classified as a II3r open cluster by Trumpler (1930), and has a diameter of about 5 arcmin, according to Lyngå (1987). It is quite an interesting object due to its shape, for which in the past it was considered a possible globular cluster, and also presents an unusual combination of age and metallicity. In fact, it is an intermediate-age open cluster, but rather metal-poor. It is a crucial object in determining the Galactic disc abundance gradient and the abundance spread at time and place in the disc.

The cluster is rather populous, and therefore it is an ideal candidate to be compared with theoretical models of stars with intermediate–low mass (Carraro & Chiosi 1994a, Carraro, Girardi & Chiosi 1999). Since in the past no detailed studies have been pursued with this aim, we decided to undertake a multicolour CCD study of the cluster, which is presented in the present paper. Moreover, this paper is the third of a series dedicated to improving the photometry of northern intermediate-age open clusters at Asiago Observatory. We have already reported elsewhere on NGC 1245 (Carraro & Patat 1994) and on NGC 7762 (Patat & Carraro 1995).

The plan of the paper is as follows. In Section 2 we summarize the previous studies on NGC 2158, while Section 3 is dedicated to presenting the observation and reduction strategies. The analysis of the CMD is performed in Section 4, and Section 5 deals with the determination of cluster reddening, distance and age. Section 6 illustrates NGC 2158 kinematics. Finally, Section 7 summarizes our findings.

2 PREVIOUS INVESTIGATIONS

NGC 2158 has been studied several times in the past. The first investigation was carried out by Arp & Cuffey (1962), who obtained photographic *BV* photometry for about 900 stars down to $V = 18.5$. Photographic photometry was also obtained by Karchenko, Andruk & Schilbach (1997) for more than 2000 stars down to the same limiting magnitude, together with proper motions.

CCD photometry in *B* and *V* passbands was provided by Christian, Heasley & Janes (1985) and Piersimoni et al. (1993). Both these studies reach deeper magnitude limits. Anyhow, the former study basically provides only a selection of main-sequence (MS) unevolved stars, whereas the latter one presents a nice CMD, but the analysis of the data appears very preliminary.

★ Based on observations carried out at Mt Ekar, Asiago, Italy. All the photometry is available at WEBDA data base: http://obswww.unige.ch/webda/navigation.html

†E-mail: giovanni.carraro@unipd.it (GC); lgirardi@pd.astro.it (LG); marigo@pd.astro.it (PM)

Table 1. Journal of observations of NGC 2158 (2000 January 6 and 7).

Field	Filter	Time integration (s)	Seeing (arcsec)
#1			
	U	240	1.2
	B	300	1.3
	V	120	1.3
	R	60	1.5
	I	120	1.3
#2			
	U	240	1.2
	B	300	1.1
	V	120	1.3
	R	60	1.5
	I	120	1.3

There is some disagreement in the literature about the values of the fundamental parameters of NGC 2158, especially the cluster age. Estimates of cluster metallicities have been obtained by several authors, and, though different, they all point to a subsolar metal content ([Fe/H] $= -0.60$; Geisler 1987; Lyngå 1987). Finally, the kinematics of NGC 2158 has been studied by measuring spectra of giant stars (Minniti 1995; Scott, Friel & Janes 1995) to provide radial velocities. It turns out that the mean cluster radial velocity is in the range 15–30 km s^{-1} (Scott et al. 1995).

3 OBSERVATIONS AND DATA REDUCTION

Observations were carried out with the AFOSC camera at the 1.82-m telescope of Cima Ekar, in the nights of 2000 January 6 and 7 (Table 1). AFOSC samples a 8.14×8.14 arcmin^2 field in a 1K × 1K thinned CCD. The typical seeing was between 1.0 and 1.5 arcsec.

For NGC 2158, typical exposure times were of 240 s in *U*, 300 s in *B*, and 60–120 s in *VRI*. Several images were taken, either centred on the cluster core, or shifted by about 4 arcmin in order to sample the neighbouring field better (see Fig. 1). However, only the images with the best seeing were used. We also observed a set of standard stars in M67 (Schild 1983; Porter, unpublished).

The data have been reduced by using the IRAF[1] packages CCDRED, DAOPHOT and PHOTCAL. The calibration equations obtained (see Fig. 2) are

$$u = U + 4.080 \pm 0.005 + (0.010 \pm 0.015)(U - B) + 0.55X,$$
$$b = B + 1.645 \pm 0.010 + (0.039 \pm 0.015)(B - V) + 0.30X,$$
$$v = V + 1.067 \pm 0.011 - (0.056 \pm 0.018)(B - V) + 0.18X,$$
$$r = R + 1.109 \pm 0.012 - (0.075 \pm 0.032)(V - R) + 0.13X,$$
$$i = I + 1.989 \pm 0.048 + (0.118 \pm 0.145)(R - I) + 0.08X, \qquad (1)$$

where *UBVRI* are standard magnitudes, *ubvri* are the instrumental ones, and *X* is the airmass. For the extinction coefficients, we assumed the typical values for the Asiago Observatory. Fig. 2 shows the residuals of the above calibration equations as a function of colour for all our standard stars.

Finally, Fig. 3 presents the run of photometric errors as a function of magnitude. These errors take into account fitting errors from DAOPHOT and calibration errors, and have been computed

[1] IRAF is distributed by the National Optical Astronomy Observatories, which are operated by the Association of Universities for Research in Astronomy, Inc., under cooperative agreement with the National Science Foundation.

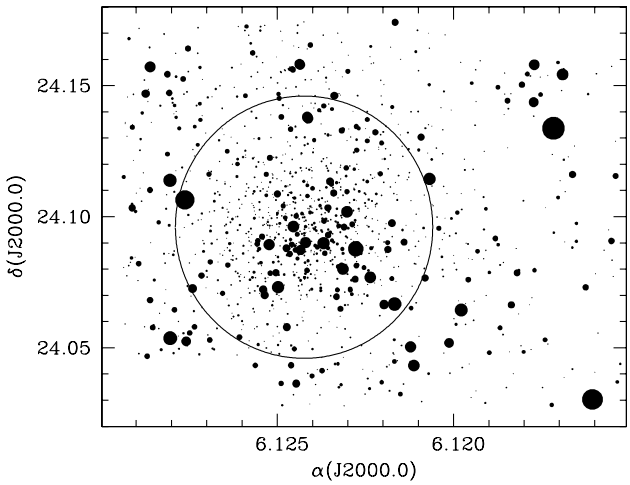

Figure 1. A *V* map of the observed field from the photometry of one of the deep *V* frames; north is up and east is to the left; the field is 9×11 arcmin^2. The circle confines the stars within 3 arcmin of the cluster centre. The size of each star is inversely proportional to its magnitude.

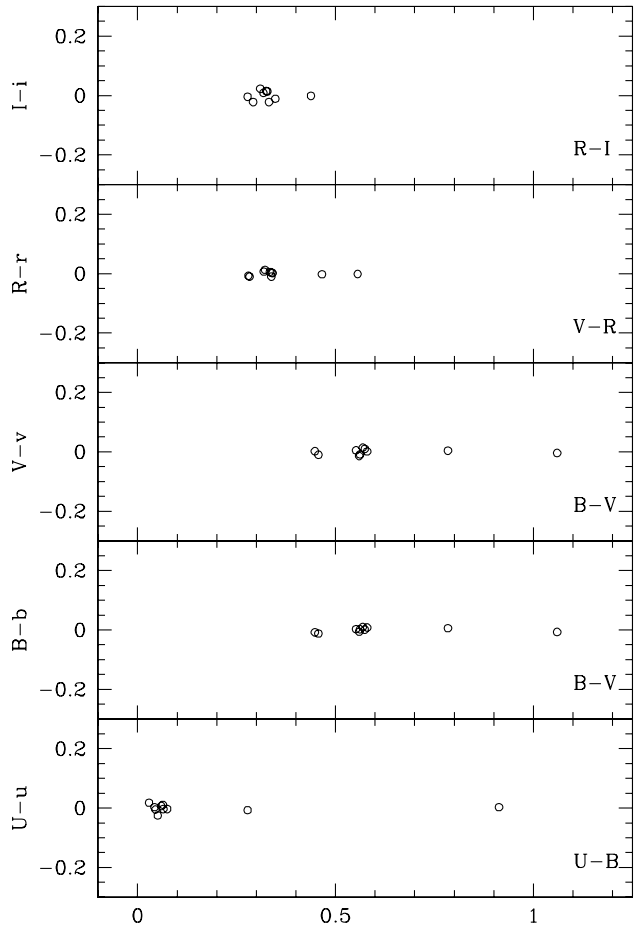

Figure 2. Differences between standard magnitudes and those obtained from equation (1) for our standard stars and as a function of colour.

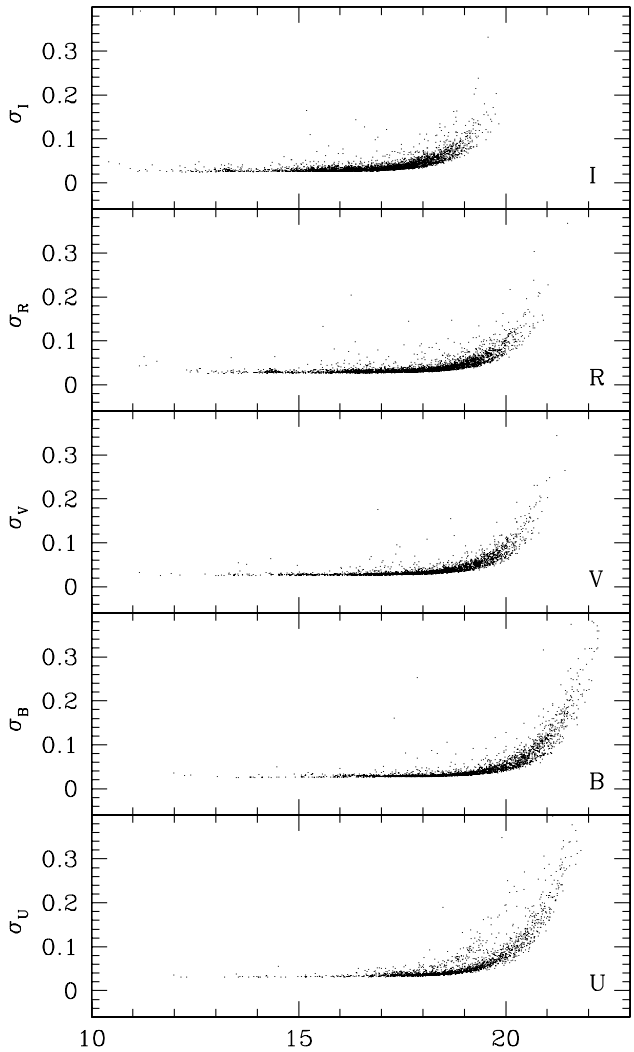

Figure 3. Photometric errors as a function of magnitude, for our NGC 2158 observations.

following Patat & Carraro (2001). It may be noticed that stars brighter than about 20 in *V*, *R* and *I*, and about 21 in *B* and *U*, have photometric errors lower than 0.1 mag. The final photometric data are available in electronic form at the WEBDA site.[2]

4 THE COLOUR–MAGNITUDE DIAGRAMS

A comparison of our photometry with past analyses is shown in Fig. 4, from which it is evident that the present study supersedes the previous ones. In fact, we reach $V = 21$, and are able to cover all the relevant regions of the CMD. The photometry by Arp & Cuffey (1962) extends only for a couple of magnitudes below the turn-off point (TO), whereas the photometry by Christian et al. (1985) does not cover the evolved region of the CMD.

To better identify the TO location and the red giant (RG) clump, in Fig. 5 we plot the CMDs obtained by considering stars located in different cluster regions. In detail, the left-hand panel presents the CMD obtained by including all the measured stars, the central panel considers the stars within a circle of radius 3-arcmin, whereas the right-hand panel presents only the stars located inside a circle of radius 1.5 arcmin. The radius adopted in the central

[2] http://obswww.unige.ch/webda/navigation.html

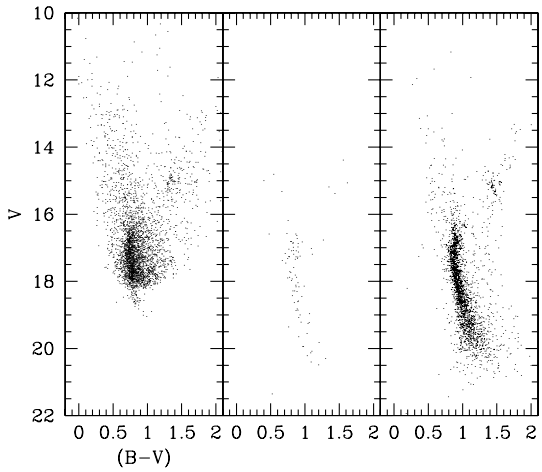

Figure 4. *BV* CMDs of NGC 2158. The left-hand panel presents the Arp & Cuffey (1962) photometry, and the central panel the Christian et al. (1985) photometry, whereas the right-hand panel shows our photometry.

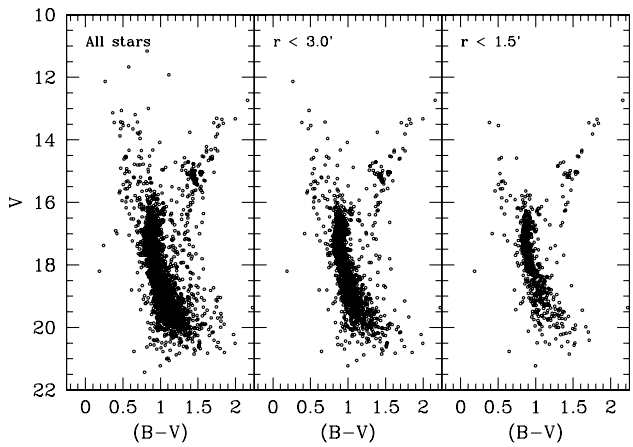

Figure 5. *BV* CMDs of NGC 2158. The left-hand panel presents the CMD obtained by including all the measured stars, the central panel considers the stars within a radius of 3 arcmin, whereas the right-hand panel shows only the stars located inside a radius of 1.5 arcmin.

panel is compatible with the available estimate of the cluster diameter, which is about 5 arcmin, so that we are probably considering most of the cluster members. By inspecting this CMD, we find that the TO is located at $V \approx 16.0$, $(B - V) \approx 1.0$, whereas a prominent clump of He-burning stars is visible at $V \approx 15.0$, $(B - V) \approx 1.5$. The diagonal structure of the latter is probably due to differential reddening effects, which we are going to discuss in Section 5.3. The MS extends for 5 mag, becoming wider at increasing magnitudes: this is compatible with the trend of photometric errors (see Fig. 3) and the probable presence of a significant population of binary stars. The global CMD morphology resembles that of NGC 7789 (Vallenari, Carraro & Richichi 2000) and NGC 2141 (Carraro et al. 2001), two well-studied rich, intermediate-age open clusters.

5 CLUSTER FUNDAMENTAL PARAMETERS

The fundamental parameters of NGC 2158 are still controversial in the literature (see Table 2). The cluster age estimates range from 0.8 to 3.0 Gyr, the distance from 3500 to 4700 pc, and the reddening $E(B - V)$ from 0.35 to 0.55. In the next sections we

Table 2. Fundamental parameters of NGC 2158 taken from the literature.

	Arp & Cuffey	Christian et al.	Kharcenko et al.	Piersimoni et al.
$E(B-V)$	0.43	0.55	0.35	0.55
$(m-M)$	14.74	14.40	13.90	15.10
distance (pc)	4700	3500	3700	4700
Age (Gyr)	0.8	1.5	3.0	1.2

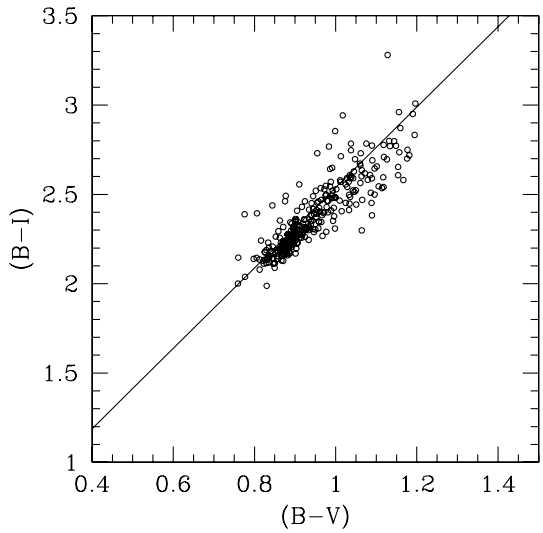

Figure 6. NGC 2158 MS stars within 3 arcmin in the $(B-V)$ versus $(B-I)$ plane.

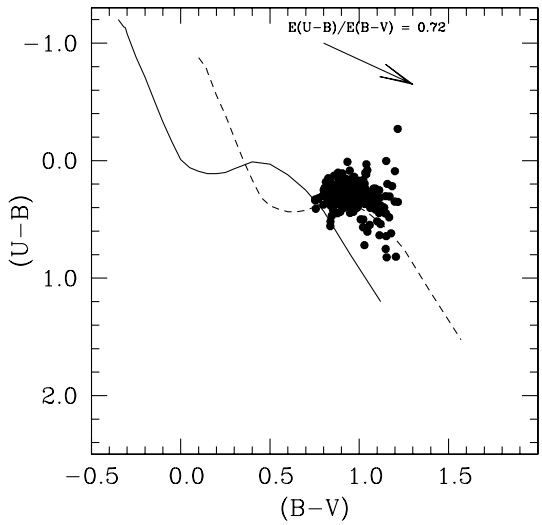

Figure 7. NGC 2158 stars within 3 arcmin in the colour–colour diagram. The solid line is an empirical ZAMS taken from Schmidt-Kaler (1982), whereas the dashed line is the same ZAMS, but shifted by $E(B-V)=0.55$. The arrow indicates the reddening law.

are going to derive update estimates for NGC 2158 basic parameters.

5.1 Reddening

In order to obtain an estimate of the cluster mean reddening, we analyse the distribution of the stars with $V<17$ in the $(B-I)$ versus $(B-V)$ plane, which is shown in Fig. 6.

The linear fit to the main sequence in the $(B-I)$ versus $(B-V)$ plane,

$$(B-I)=Q+2.25\times(B-V), \tag{2}$$

can be expressed in terms of $E(B-V)$, for the $R_V=3.1$ extinction law, as

$$E(B-V)=\frac{Q-0.014}{0.159}, \tag{3}$$

following the method proposed by Munari & Carraro (1996a,b). This method provides a rough estimate of the mean reddening and, as amply discussed in Munari & Carraro (1996a), it can be used only for certain colour ranges. In particular, equation (3) holds over the range $-0.23\le(B-V)_0\le+1.30$. MS stars have been selected by considering all the stars within 3 arcmin of the cluster centre and having $17\le V\le 21$ and $0.75\le(B-V)\le 1.25$. A least-squares fit through all these stars gives $Q=0.097$, which, inserted in equation (3), provides $E(B-V)=0.56\pm0.17$. The uncertainty is rather large, and is due to the scatter of the stars in this plane, which indicates the presence of stars with different reddening, presumably a mixture of stars belonging to the cluster and to the field.

Another indication of the cluster mean reddening can be derived from the colour–colour diagram $(U-B)$ versus $(B-V)$, shown in Fig. 7. Here we consider again all the stars located within 3 arcmin of the cluster centre having $17\le V\le 21$ and $0.75\le(B-V)\le 1.25$, to alleviate the contamination effect. The solid line is an empirical zero-age main sequence (ZAMS) taken from Schmidt-Kaler (1982), whereas the dashed line is the same ZAMS, but shifted by $E(B-V)=0.55$. The ratio $E(U-B)/E(B-V)=0.72$ has been adopted. This shift, together with the dispersion of the data around the shifted ZAMS, provides the reddening value of $E(B-V)=0.55\pm0.10$.

5.2 Distance and age

As already mentioned, there is still a considerable dispersion in the literature among different estimates of NGC 2158 distance and age. We have derived new estimates for these parameters as follows.

First, from the Girardi et al. (2000a) data base we generate theoretical isochrones of metallicity $Z=0.0048$, which corresponds to the observed value of [Fe/H] $=-0.60$. Fig. 8 shows the isochrones with ages between 1.58 to 2.51 Gyr, which defines the age interval compatible with the observed magnitude difference between the red clump and the turn-off region. The isochrones were shifted in apparent magnitude and colour, until the locus of core-helium burning stars coincided with the observed mean position of the clump. The results, shown in Fig. 8, imply a true distance modulus of $(m-M)_0=12.8$ mag (3630 pc), and a colour excess of $E(B-V)=0.60$, for NGC 2158. The latter value is compatible with that obtained in Section 5.1.

It should be remarked that these are just first estimates of the

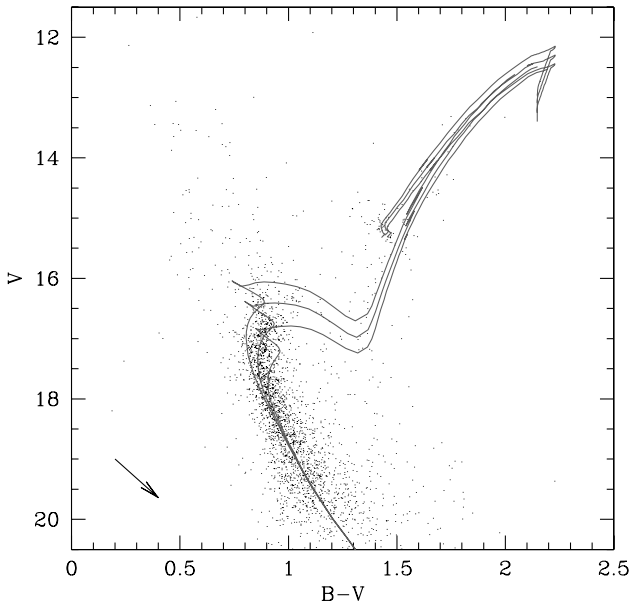

Figure 8. NGC 2158 data the V versus $B-V$ diagram (points), as compared to Girardi et al. (2000a) isochrones of ages 1.58×10^9, 2.00×10^9 and 2.51×10^9 yr (solid lines), for the metallicity $Z=0.0048$. A distance modulus of $(m-M)_0=12.8$, and a colour excess of $E(B-V)=0.60$, have been adopted. The direction of the reddening vector is indicated by the arrow at the bottom left.

cluster parameters, which we will now try to test further by means of synthetic CMDs. Fig. 9 shows the sequence of steps required to simulate a CMD aimed to reproduce the NGC 2158 data. These steps are as follows.

(1) The 2-Gyr-old isochrone of $Z=0.0048$ is used to simulate a cluster with 100 red clump stars. Assuming a Kroupa (2001) IMF, in order to reach this number we need an initial cluster mass of about $1.5\times10^4\,M_\odot$, which is assumed hereinafter. We have simulated detached binaries, assuming that 30 per cent of the observed objects are binaries with a mass ratio located between 0.7 and 1.0. This prescription is in agreement with several estimates for galactic open clusters (Carraro & Chiosi 1994a,b) and with the observational data for NGC 1818 and 1866 in the LMC (Elson et al. 1998; Barmina, Girardi & Chiosi 2001). The result of such a simulation is shown in Fig. 9(a). In this panel we can see that most of the stars – the single ones – distribute along the very thin sequence defined by the theoretical isochrone. Binaries appear as both (i) a sequence of objects roughly parallel to the main sequence of single stars, and (ii) some more scattered objects in the evolved part of the CMD.

(2) In order to estimate the location of foreground and background stars, we use a simple Galaxy model code (Girardi et al., in preparation). It includes the several Galactic components – thin and thick disc, halo, and an extinction layer – adopting geometric parameters as calibrated by Groenewegen et al. (2001) . The most relevant component in this case is the thin disc, which is modelled by exponential density distributions in both vertical and radial directions. The radial scaleheight is kept fixed (2.8 kpc), whereas the vertical scaleheight h_z increases with the stellar age t as

$$h_z = z_0(1+t/t_0)^\alpha, \qquad (4)$$

with $z_0=95$ pc, $t_0=4.4$ Gyr, and $\alpha=1.66$. The simulated field has the same area (9×11 arcmin^2) and galactic coordinates ($\ell=186\overset{\circ}{.}64$, $b=+1\overset{\circ}{.}80$) as the observed one for NGC 2158. The results are shown in Fig. 9(b). It is noteworthy that, in this direction, most of the Galactic field stars appear in a sort of diagonal sequence in the CMD that roughly corresponds to the position of NGC 2158 main sequence.

(3) We then simulate the photometric errors as a function of V magnitude, with typical values derived from our observations (see Fig. 3). The results are shown separately for cluster and field stars in panels (c) and (d) of Fig. 9.

(4) The sum of field and cluster simulations is shown in Fig. 9(e). This can be compared directly to the observed data, shown in Fig. 9(f).

The comparison of these last two panels indicates that the selected cluster parameters – age, metallicity, mass, distance, reddening, and binary fraction – really lead to an excellent description of the observed CMD, when coupled with the simulated Galactic field. The most noteworthy aspects of this comparison are the location and shape of the turn-off and subgiant branch, which are the features most sensitive to the cluster age.

Of course, there are minor discrepancies between the observed and simulated data. (i) The simulated cluster is better delineated in the CMD than the data. This may be ascribed to a possible underestimate of the photometric errors in our simulations, and to the possible presence of differential reddening across the cluster (see next section). (ii) There is a deficit of simulated field stars, which can be noticed more clearly for $V<16$ and $(B-V)<1$. This is caused by the simplified way in which the thin disc is included in the Galactic model: it is represented by means of simple exponentially decreasing stellar densities in both radial and vertical directions, and does not include features such as spiral arms, intervening clusters, etc., that are necessary to correctly describe fields at low galactic latitudes. Anyway, the foreground/ background simulation we present is only meant to give us an idea of the expected location of field stars in the CMD.

Although these shortcomings in our simulations might probably be eliminated with the use of slightly different prescriptions, they do not affect our main results, namely the choice of cluster parameters.

We therefore conclude that $(m-M)_0=12.8$ mag (3630 pc), $E(B-V)=0.60$, age 2 Gyr, $Z=0.0048$ ([Fe/H] $=-0.60$), and mags $1.5\times10^4\,M_\odot$ well represent the cluster parameters. All these values are uncertain to some extent.

(1) From Fig. 8, we can estimate a maximum error of 15 per cent (0.3 Gyr) in the age. One should keep in mind, however, that the absolute age value we derived, of 2 Gyr, depends on the choice of evolutionary models, and especially on the prescription for the extent of convective cores. For the stellar masses envolved ($M_{TO}\sim1.5\,M_\odot$ for NGC 2158), our models (Girardi et al. 2000a) include a moderate amount of core overshooting.

(2) Our best-fitting model corresponds to $E(B-V)=0.60$, which is compatible with the range $E(B-V)=0.55\pm0.1$ indicated in Section 5.1. The uncertainty of 0.1 mag in $E(B-V)$ causes an uncertainty of ~0.3 mag in the distance modulus (15 per cent in distance).

(3) The metallicity cannot be better constrained from the CMD data, unless we have more accurate estimates of the reddening.

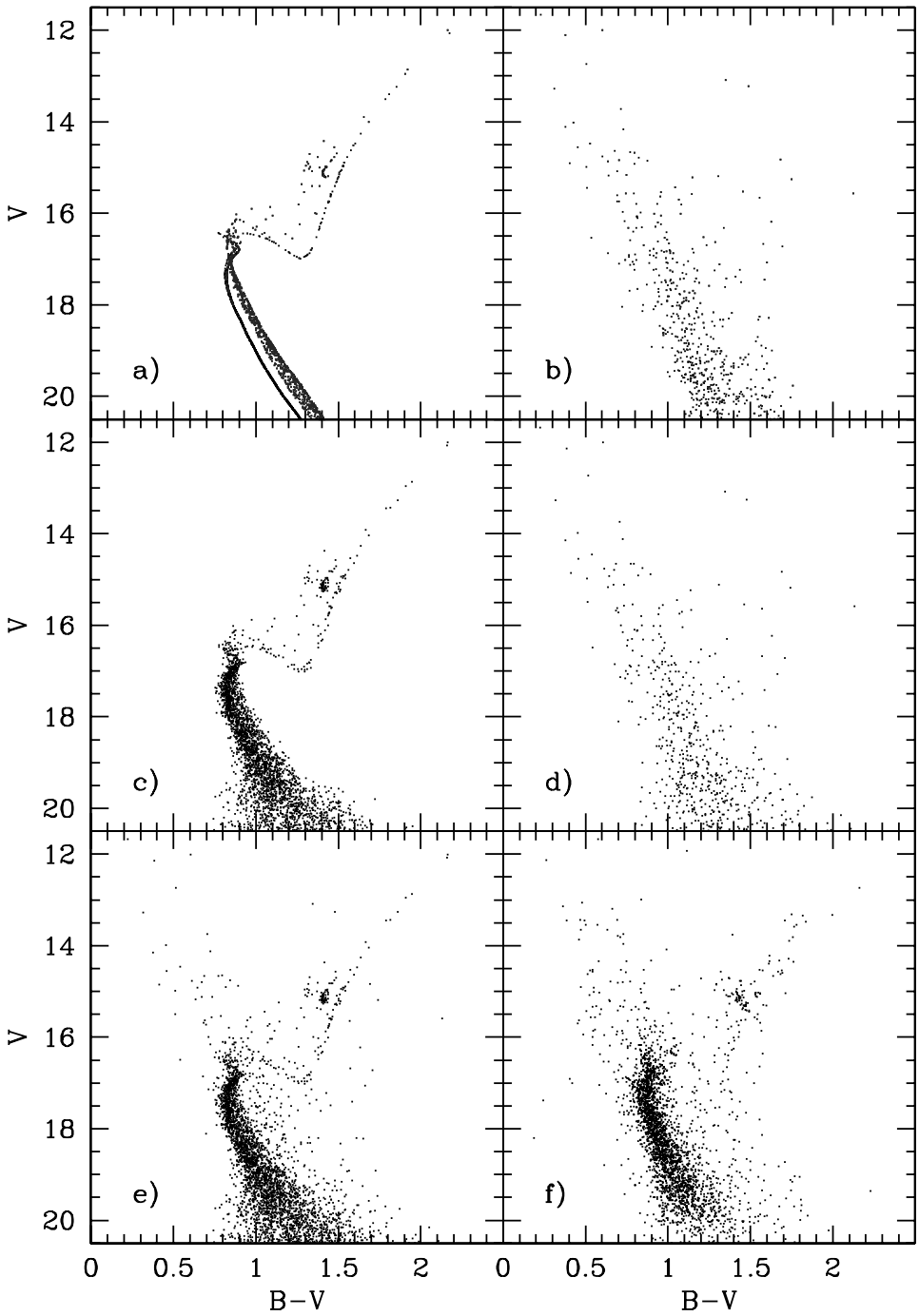

Figure 9. Simulations of NGC 2158 and its field in the V versus $B-V$ diagram. **(a)** Simulation of a 2-Gyr-old cluster with $Z = 0.0048$ and a initial mass of $1.5 \times 10^4\,M_\odot$, based on the same isochrones, distance modulus and colour excess as in Fig. 8. We have assumed that 30 per cent of the stars are binaries with mass ratios between 0.7 and 1.0. **(b)** Simulation of a 9×11 arcmin^2 field centred at galactic coordinates $\ell = 186\overset{\circ}{.}64$, $b = +1\overset{\circ}{.}80$, performed with Girardi et al. (2002) Galactic model. Panels **(c)** and **(d)** are the same as (a) and (b), respectively, after simulation of photometric errors. Panel **(e)** shows the sum of (c) and (d), which can be compared to the observational data shown in panel **(f).**

(4) The initial mass estimate depends heavily on the choice of IMF, which determines the mass fraction locked into low-mass (unobserved) objects. The value of $1.5 \times 10^4\,M_\odot$ was obtained with a Kroupa (2001) IMF, corrected in the lowest mass interval according to Chabrier (2001; details are given in Groenewegen et al. 2001), and should be considered just as a first guess. At present ages, supernovae explosions and stellar mass loss would have reduced this mass by about 20 per cent.

5.3 Red clump structure and differential reddening

Our cluster simulations also allows us to examine in more detail the observed structure of the red clump in NGC 2158. Fig. 10 details the clump region in the CMD, for both simulations (panels a and b) and data (panel c). As can be readily noticed in panel (c), the observed clump appears as a diagonal structure, whose slope is roughly coincident with the reddening vector. In cluster

simulations, however, the clump is normally seen as a more compact structure. This can be appreciated in the simulations for single stars shown in Girardi, Mermilliod & Carraro (2000b), where the model clumps are found to be more elongated in the top–bottom direction in the CMD, and not diagonally. The same result is found in Fig. 10(a), if we look only at the locus of single stars.

However, part of the clump widening might be caused by the presence of binaries, as shown by the different symbols in our simulations of panels (a) and (b). It turns out that binaries composed of clump plus turn-off stars are located at a bluer colour, and are slightly brighter, if compared to the locus of single clump stars. Thus, binaries tend to widen the clump structure along a direction that roughly coincides with the reddening vector. Nevertheless, as can be readily noticed from Fig. 10, binaries cannot account entirely for the clump elongation observed in NGC 2158.

Instead, since NGC 2158 is located very close to the Galactic plane, the observed clump morphology might well be caused by the presence of differential reddening over the cluster. We can get an estimate of the expected differential reddening, starting from simple models of the dust distribution in the thin disc. For this purpose, we use the Girardi et al. (2001) Galactic model, assume a local extinction value of $0.75\,\mathrm{mag\,kpc^{-1}}$ in V (Lyngå 1982), and a diffuse dust layer of exponentially decreasing density with a scaleheight equal to 110 pc. With these parameters, in correspondence with the NGC 2158 location we obtain a differential reddening of $\Delta E(B-V)/\Delta b = -0.021\,\mathrm{mag\,arcmin^{-1}}$ perpendicular to the Galactic plane. This estimate has the right order of magnitude to explain the width of the observed clump.

In order to investigate whether this kind of picture is realistic, in Fig. 11 we plot the CMDs for NGC 2158, separated in different strips of Galactic latitude b. The 2-Gyr-old isochrone, located at a fixed position in all panels, allows an easy visualization of how the clump gets bluer at increasing b.[3] Assuming that this effect is caused by differential reddening perpendicular to the Galactic plane, we get an estimate of $\Delta E(B-V)/\Delta b \simeq -0.011\,\mathrm{mag\,arcmin^{-1}}$.

We conclude that NGC 2158 presents some amount of differential reddening. Along the ∼6-arcmin diameter of the cluster, this effect amounts to about $\Delta E(B-V) \sim 0.06$ mag. Since our previous determinations of the cluster age, distance and reddening were based on the mean location of the observed stars, the correction of the data for differential reddening would not imply any significant change in the derived parameters.

6 CLUSTER KINEMATICS

The availability of mean radial velocity and proper motion measurements allows us to discuss in some detail the kinematics of NGC 2158. Radial velocity has been measured for eight stars by Scott et al. (1995) and for 20 stars by Minniti (1995). These measurements have a comparable accuracy between 10 and $15\,\mathrm{km\,s^{-1}}$. A systematic shift of about $10\,\mathrm{km\,s^{-1}}$ is likely to exist, in the sense that the mean radial velocity from Minniti (1995) is lower than that derived by Scott et al. (1995). Although the Minniti (1995) mean radial velocity is based on better statistics, we shall present results based upon both the determinations.

Absolute proper motions have been derived by Kharchenko et al.

[3] A similar effect was also noticed for NGC 2158 main-sequence stars.

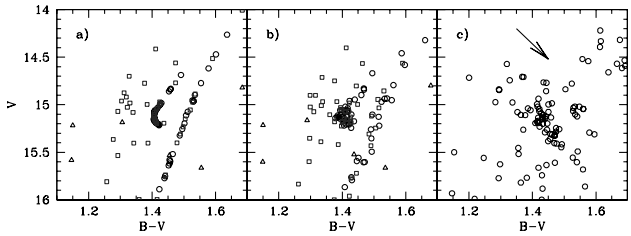

Figure 10. The same simulations as in Fig. 9, but detailing the region of clump giants. **(a)** The simulated data. Circles are single stars in the cluster, squares are the binaries, and the few triangles are field stars. **(b)** The same as in panel (a), but including the simulation of photometric errors. **(c)** The observed data for NGC 2158. The arrow shows the reddening vector corresponding to $\Delta E(B-V) = 0.1$.

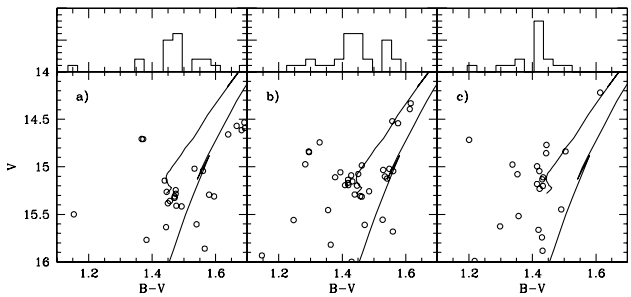

Figure 11. Bottom panels: The same as in Fig. 10, but now illustrating the stellar data at different intervals of galactic latitude, namely **(a)** $1\overset{\circ}{.}73 < b < 1\overset{\circ}{.}77$ (toward NE in Fig. 1), **(b)** $1\overset{\circ}{.}77 < b < 1\overset{\circ}{.}81$ (central part of the cluster), and **(c)** $1\overset{\circ}{.}81 < b < 1\overset{\circ}{.}85$ (toward SW). In all cases, only stars located at $186\overset{\circ}{.}58 < \ell < 186\overset{\circ}{.}69$ (a strip about 7 arcmin wide) were plotted. As a reference to the eye, we also plot the same 2-Gyr-old isochrone as shown in Fig. 8. The panels at the top illustrate, for each case, the colour histogram of stars with $14.7 < V < 15.7$. Notice the progressive shift of the clump to the blue as b increases.

(1997), and amount to $\mu_x = +0.66 \pm 2.03$, $\mu_y = -3.23 \pm 2.16$, where $\mu_x = \mu_\alpha \times \cos\delta$ and $\mu_y = \mu_\delta$.

Following in detail Carraro & Chiosi (1994b) and Barbieri & Gratton (2001), we derived the velocity components of NGC 2158 in a Galactocentric reference frame U, V and W. The results are summarized in Table 3.

By adopting the Allen & Santillán (1991) rotationally symmetric Galaxy mass model, we integrated back in time NGC 2158 orbit for a duration comparable with NGC 2158 age (see Section 5.2), in order to obtain estimates of its eccentricity, epiciclycal (ω-) and vertical (z-) amplitude. These parameters, together with age and metallicity, are fundamental to place the cluster in the right disc population.

The orbit integration has been performed using a modified version of the second-order Burlish–Stoer integrator originally developed by S. J. Aarseth (private communication). We provide orbits both for the Minniti (1995) and Scott et al. (1995) mean radial velocity estimates. They are shown in the upper and middle panels of Fig. 12. The parameters are basically consistent, as listed also in Table 4. For the sake of the discussion, in the lower panel we show a new orbit determination for the open cluster NGC 2420, which roughly shares the same age (1.8 Gyr) and metallicity ([Fe/H] = −0.42) of NGC 2158 (Friel & Janes 1993; Carraro et al 1998). The orbit of NGC 2420 was previously computed by Keenan & Innanen (1974), who suggest that this cluster might have been disturbed in his motion around the Galactic Centre by the influence of the Magellanic Clouds, a hypothesis which sounds

Table 3. NGC 2158 basic kinematical parameters. The velocity components have been computed by adopting Minniti (1995, first row) Scott et al. (1995, second row) radial velocity estimates.

$(m-M)_0$	X kpc	Y kpc	Z kpc	U km s^{-1}	V km s^{-1}	W km s^{-1}
12.80	12.11	−0.42	0.11	−7.99	−56.50	−16.88
				−21.88	−58.13	−16.45

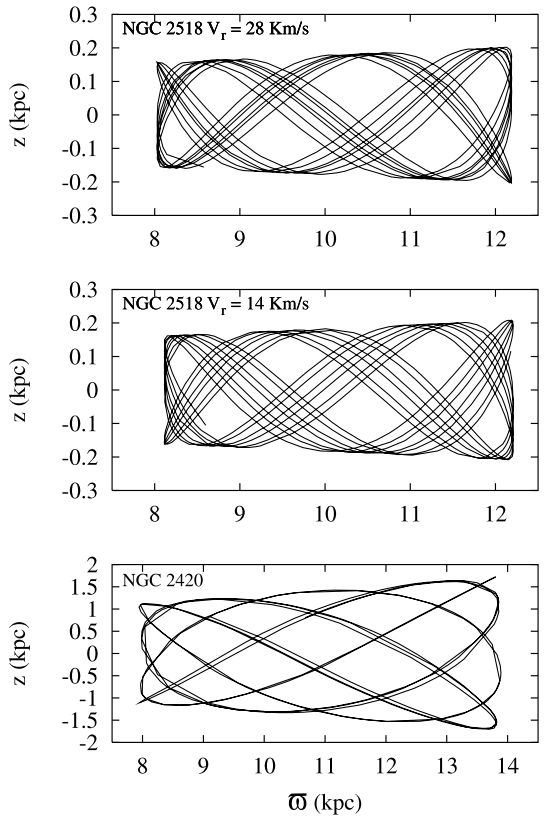

Figure 12. The orbit of NGC 2158 in the meridional plane. In the top panel we display the orbit obtained by using the radial velocity estimate from Scott et al. (1995), whereas the middle panel shows the orbit obtained by adopting the radial velocity estimate from Minniti (1995). The bottom panel presents the orbit of NGC 2420.

reasonable – the cluster has high eccentricity, large apogalacticon and stays most of the time relatively high above the Galactic plane – but which deserves a further detailed numerical investigation.

Christian et al. (1985) argue about the possibility that NGC 2158 and 2420 might share common properties and origin, since they are coeval and have very low metal abundances for open clusters of this age. It is therefore interesting to compare their orbits, also because NGC 2158 is even metal-poorer than NGC 2420. With an eccentricity $e = (R_a - R_p)/(R_a + R_p) = 0.20$ – where R_a and R_p are the apo- and peri-galacticon, respectively – the cluster reaches a maximum distance of about 12 kpc from the Galactic Centre in the direction of the anticentre, where it is located right now and where it probably formed. It remains relatively low in the Galactic disc, in a region populated by young and intermediate-age Population I objects. The only difference with this population is the rather low metal content, less than half the solar value.

Table 4. Basic parameters of the orbit of NGC 2158.

	R_a kpc	R_p kpc	e	z_{max} kpc
Minniti	12.21	8.11	0.20	0.21
Scott et al.	12.19	8.03	0.21	0.20

Apparently, we are facing two significantly different orbits. NGC 2158 has an orbit more similar to normal Population I objects, whereas NGC 2420 possesses an eccentricity much higher than the typical Population I objects. Moreover, NGC 2420 is more distant than NGC 2158. NGC 2420 and 2158 are not the only cases of low metallicity, intermediate-age clusters in the anticentre direction. From Carraro, Ng & Portinari (1998) we have extracted 11 open clusters with ages between 1.5 and 3.5 Gyr and low metal content ([Fe/H] < -0.50). All these clusters presently lie in a Galactic sector between $\ell = 135°$ and $\ell = 225°$. They are: NGC 2158, NGC 2204, NGC 2420, NGC 2141, NGC 2243, Tombaugh 2, Berkeley 19, 20, 21, 31 and 32. The common properties of these clusters suggest the possibility that they formed from the same material. Typically, the mean metal content of the Galactic disc at distances between 12 and 16 kpc ranges between [Fe/H] $= -0.50$ and [Fe/H] $= -0.70$, according to recent estimates of the Galactic disc metallicity gradient (Carraro et al. 1998). Such a low metal content is compatible with the low density, hence low star formation, probably typical of that region. In this respect it would be interesting to compute Galactic orbits for all these clusters to check whether a trend exists to have more eccentric orbits at increasing Galactocentric distance in this region of the anticentre. This would promote a better understanding of the structure and evolution of the outer Galactic disc.

7 CONCLUSIONS

We have presented a new CCD *UBVRI* photometric study of the intermediate-age open cluster NGC 2158. From the analysis of the available data we can draw the following conclusions:

(1) the age of NGC 2158 is about 2 Gyr, with a 15 per cent uncertainty;

(2) the reddening $E(B-V)$ turns out to be 0.55 ± 0.10, and we find evidence of differential reddening (of about 0.06 mag) across the cluster;

(3) we place the cluster at about 3.6 kpc from the Sun toward the anticentre direction, and

(4) combining together NGC 2158 age, metallicity and kinematics, we suggest that it is a genuine member of the old thin disc population.

ACKNOWLEDGMENTS

We are very grateful to Chiara Miotto for carefully reading this manuscript, to Mauro Barbieri for the NGC 2158 orbit integration, to Martin Groenewegen for the latest calibration of the Galactic model, and to Luciano Traverso, who secured the observations of January 7. We also acknowledge the referee, Dr G. Gilmore, for his useful suggestions. This study has been financed by the Italian Ministry of University, Scientific Research and Technology (MURST) and the Italian Space Agency (ASI), and made use of Simbad and WEBDA data bases.

REFERENCES

Allen C., Santillán A., 1991, Rev. Mex. Astron. Astrofis., 22, 255
Arp H., Cuffey J., 1962, ApJ, 136, 51
Barbieri M., Gratton R. G., 2001, A&A, in press
Barmina R., Girardi L., Chiosi, 2001, A&A, in press
Carraro G., Chiosi C., 1994a, A&A, 287, 761
Carraro G., Chiosi C., 1994b, A&A, 288, 751
Carraro G., Patat F., 1994, A&A, 289, 397
Carraro G., Ng Y. K., Portinari L., 1998, MNRAS, 296, 1045
Carraro G., Girardi L., Chiosi C., 1999, MNRAS, 309, 430
Carraro G., Hassan S. M., Ortolani S., Vallenari A., 2001, A&A, 372, 879
Chabrier G., 2001, ApJ, 554, 1274
Christian C. A., Heasley J. N., Janes K. A., 1985, ApJ, 299, 683
Elson R. A. W., Sigurdsson S., Davies M., Hurley J., Gilmore G., 1998, MNRAS, 300, 857
Friel E. D., Janes K. A., 1993, A&A, 267, 75
Geisler D., 1987, AJ, 94, 84
Girardi L., Bressan A., Bertelli G., Chiosi C., 2000a, A&AS, 141, 371
Girardi L., Mermilliod J.-C., Carraro G., 2000b, A&A, 354, 892
Girardi L. et al., 2002, A&A, submitted
Groenewegen M. A. T. et al., 2001, A&A, submitted
Keenan D. W., Innanen K. A., 1974, ApJ, 189, 205
Kharcenko N., Andruk V., Schilbach E., 1997, Astron. Nach., 318, 253
Kroupa P., 2001, MNRAS, 322, 231
Lyngå G., 1982, A&A, 109, 213
Lyngå G., 1987, The Open Star Clusters Catalogue, 5th edition (http://cdsweb.u-strasbg.fr/htbm/cats/VII/92A)
Minniti D., 1995, A&AS, 113, 299
Munari U., Carraro G., 1996a, A&A, 314, 108
Munari U., Carraro G., 1996b, MNRAS, 283, 905
Patat F., Carraro G., 1995, A&AS, 114, 281
Patat F., Carraro G., 2001, MNRAS, 325, 1591
Piersimoni A., Cassisi S., Brocato E., Straniero O., 1993, Mem. Soc. Astron. Ital., 64, 609
Schild R. E., 1983, PASP, 95, 1021
Schmidt-Kaler Th., 1982, in Schaifers K., Voigt H. H., eds, Landolt-Börnstein, Numerical data and Functional Relationships in Science and Technology, New Series, Group VI, Vol. 2(b). Springer Verlag, Berlin, p. 14
Scott J. E., Friel E. D., Janes K. A., 1995, AJ, 109, 1706
Trumpler R. J., 1930, Lick Obs. Bull., 14, 154
Vallenari A., Carraro G., Richichi A., 2000, A&A, 353, 147

This paper has been typeset from a TEX/LATEX file prepared by the author.